MCB
Journals.ASM.org

The Phosphatase-Transcription Activator EYA1 Is Targeted by Anaphase-Promoting Complex/Cdh1 for Degradation at M-to-G_1 Transition

Jianbo Sun,[a] Zoi Karoulia,[a] Elaine Y. M. Wong,[a] Mohi Ahmed,[a] Keiji Itoh,[b] Pin-Xian Xu[a,b]

Department of Genetics and Genomic Sciences[a] and Developmental and Regenerative Biology,[b] Mount Sinai School of Medicine, New York, New York, USA

The phosphatase and transactivator EYA family proteins are overexpressed in many cancer cell lines and are abundantly distributed in undifferentiated cells during development. Loss-of-function studies have shown that EYA1 is required for cell proliferation and survival during mammalian organogenesis. However, how EYA1 is regulated during development is unknown. Here, we report that EYA1 is regulated throughout the cell cycle via ubiquitin-mediated proteolysis. The level of EYA1 protein fluctuates in the cell cycle, peaking during mitosis and dropping drastically as cells exit into G_1. We found that EYA1 is efficiently degraded during mitotic exit in a Cdh1-dependent manner and that these two proteins physically interact. Overexpression of Cdh1 reduces the protein levels of ectopically expressed or endogenous EYA1, whereas depletion of Cdh1 by RNA interference stabilizes the EYA1 protein. Together, our results indicate that anaphase-promoting complex/cyclosome (APC/C)–Cdh1 specifically targets EYA1 for degradation during M-to-G_1 transition, failure of which may compromise cell proliferation and survival.

The eyes absent (EYA) family proteins is composed of four members (EYA1 to EYA4) defined by a conserved C-terminal Eya domain, which interacts with other proteins and has an intrinsic phosphatase activity (1–3). The EYA proteins possess a transactivation domain in their N-terminal regions (4) and act as transcriptional coactivators by interacting with DNA-binding proteins, such as the homeodomain SIX family proteins, to transactivate genes that are essential for normal development during mammalian organogenesis (4–7). Mutations in the human *EYA1* cause branchio-oto-renal (BOR) and branchio-oto (BO) syndromes, which are characterized by branchial arch abnormalities and hearing loss with or without kidney defects (8–11). Deletion of either gene in mice results in the absence of the inner ear, kidney, and thymus as well as reduction of other tissues (10, 12, 13).

During mouse embryonic development, *Eya1* is expressed in early progenitor cells in several organ primordia and regulates cell proliferation and survival, as its inactivation in mice leads to reduced proliferation and increased apoptosis in several organ primordia (10, 12–15). In *Drosophila*, overexpression of EYA results in overproliferation, while their loss leads to tissue reduction (7, 16). Recent studies have found that the levels of EYA proteins are elevated in several cancer cells (17–20). While a recent study reported that EYA may promote DNA repair by dephosphorylating histone γH2AX (21), how EYA acts to regulate cell proliferation and its precise mode of action in cell cycle regulation remain largely unknown. Furthermore, although the biochemical functions of EYA proteins and the spatiotemporal expression pattern of their mRNAs during mouse development have been well studied, it is currently unknown how the levels of EYA proteins are regulated during development.

Most eukaryotic cell cycle regulators require targeted degradation to maintain the highly ordered series of events necessary for proper progression through each of the cell cycle stages by ubiquitin-dependent proteolysis, which depends on the recognition of substrates by E3 enzymes (22, 23). From late mitosis through early G_1, the anaphase-promoting complex/cyclosome (APC/C)-mediated ubiquitin-proteasome system is essential for cell cycle-relevant proteolytic degradation in order to exit mitosis, and its activity is targeted to appropriate substrates by evolutionarily conserved coactivators Cdc20 and Cdh1 (24). APC/C-mediated degradation occurs in two sequential waves, the first of which is coordinated by Cdc20 in mitosis (25) and the second by Cdh1 during the mitotic exit (26). Although a previous study has reported that EYA1 serves as a substrate for sumoylation with SUMO1 (small ubiquitin-related modifier) in palate development (27), it remains unclear whether its sumoylation is linked to its degradation or whether it is regulated during cell cycle progression.

Here, we set out to study EYA1 function through analysis of the regulation of EYA1 at the posttranscriptional level during the cell cycle. We found that EYA1 is ubiquitinated and the protein levels fluctuate throughout the cell cycle, being highest at mitosis. Our results demonstrate that EYA1 is targeted by the APC/C-Cdh1-mediated ubiquitin-proteasome pathway both *in vitro* and *in vivo* for degradation during the M-to-G_1 transition.

MATERIALS AND METHODS

Plasmids and mutagenesis. The Flag-tagged full length of the *Eya1* cDNA expression plasmid (*Flag-Eya1*) as well as the Flag-tagged *Eya1* domain (*Flag-Eya1D*) and *Eya1* N-terminus sequence (*Flag-Eya1N*) were previously described (9). *3×Flag-Eya1/pcDNA3* was generated by adding two additional 2× Flag tags by using a PCR method. Then 2× hemagglutinin (HA) tags were added into *3×Flag-Eya1/pcDNA3* by the same method. A QuikChange site-directed mutagenesis kit (Stratagene) was used to generate the O-box and D-box mutants in *2×HA-3×Flag-Eya1/pcDNA3*.

Received 17 November 2012 Returned for modification 10 December 2012
Accepted 13 December 2012
Published ahead of print 21 December 2012
Address correspondence to Pin-Xian Xu, pinxian.xu@mssm.edu.
J.S. and Z.K. contributed equally to this article.
Copyright © 2013, American Society for Microbiology. All Rights Reserved.
doi:10.1128/MCB.01516-12

3×Flag-Eya1-IRES-GFP-pCDNA3 was obtained by inserting the internal ribosomal entry site-green fluorescent protein (IRES-GFP) cassette into *3×Flag-Eya1/pcDNA3*. *HA-ubiquitin/pCMV* (kindly provided by L. Zhu at Albert Einstein Medical Center), *Myc-Cdh1*, and *Myc-Cdc20* expression plasmids (kindly provided by M. W. Kirschner, Harvard Medical School) were also used for this study.

Cell culture and transfections. HEK293 cells, NIH 3T3 mouse embryonic fibroblast cells (MEFs), C2C12 mouse myoblast cells, and HeLa cells were cultured according to standard protocols. The proteasome was inhibited by culturing cells for 6 h in the presence of 50 μM MG132 (Sigma) dissolved in dimethyl sulfoxide (DMSO). The concentration of cycloheximide was 0.1 mg/ml. Transient transfections were performed using Lipofectamine 2000 (Invitrogen) according to the manufacturer's instructions.

B22 cell line stably expressing Eya1. The *3×Flag-Eya1-IRES-GFP* stable cell line was developed by cotransfecting HEK293 cells with *3×Flag-Eya1-IRES-GFP/pCDNA3* and pBABE. Stable transfectants were selected for 4 weeks in the presence of 3 μg/ml puromycin. Surviving clones were analyzed by Western blotting to select *Eya1*-expressing clones.

Cell synchronization. To synchronize cells at mitotic phase, cells were treated with 100 ng/ml nocodazole for 18 h. A mitotic shake off was performed, and the cells were reseeded in complete medium for release from the arrest. The analysis of the cell cycle was performed by flow cytometry. Synchronized cells were harvested at set release time points, fixed in 70% ethanol, washed with phosphate-buffered saline (PBS), and then treated with propidium iodide (PI) staining solution (0.1% [vol/vol]), Triton X-100, 10 μg/ml of PI, and 100 μg/ml of DNase-free RNase A in PBS. The stained cells were then subjected to fluorescence-activated cell sorter (FACS) flow cytometry. Cell cycle distribution was analyzed with Flow Jo software.

CoIP, Western blotting, immunostaining, and RNA interference. Whole-cell lysates were prepared with Nonidet P-40 lysis buffer (150 mM sodium chloride, 1.0% NP-40, 50 mM Tris, pH 8.0, 1× complete protease inhibitor cocktail), and coimmunoprecipitation (coIP) was performed as described previously (9).

Antibodies used for immunoprecipitation and Western blotting were anti-cyclin A and anti-β-actin (Santa Cruz), anti-EYA1 antibody (ProSci Incorporated), anti-Flag M2 antibody and anti-Flag M2 affinity gel (Sigma), anti-HA and anti-Myc (Abcam), and anti-Fizzy-Related (FZR) antibody (Invitrogen).

For immunofluorescence staining, fluorescein isothiocyanate (FITC)-conjugated anti-α-tubulin and Cy3-conjugated secondary antibodies were used for detection. Hoechst was used for detecting nuclei.

For RNA interference, either *FZR/Cdh1* short hairpin RNA (shRNA) (sc-145283-SH; Santa Cruz), *Eya1* shRNA, or control shRNA (plasmid 1864; Addgene) was cotransfected with *2×HA-3×Flag-Eya1* into 3T3 or C2C12 cells, and cell lysates were prepared 48 h posttransfection.

RT-PCR. For reverse transcription-PCR (RT-PCR), RNAs were extracted using TRIzol reagent (Invitrogen) by following the manufacturer's protocol. First-strand cDNA was synthesized from 0.5 μg total RNA using an ImProm-II reverse transcription system (Promega) in a final 25-μl reaction mixture, and 1 μl of RT product was used as a template for PCR. *Eya1* was amplified with primers Eya1F8, 5′-TTGGAAGAGATGGCTTTCCT-3′, and Eya1R8, 5′-TATTGGAAACACAATTCCT-3′. 18S rRNA was amplified with primers 5′-TCAAGAACGAAAGTCGGAGG-3′ and 5′-GGACATCTAAGGGCATCACA-3′. Reactions were amplified and resolved on a 1.5% agarose gel in triplicate and repeated three times. *Eya1* mRNA level was normalized by the 18S rRNA reverse transcription level after being analyzed with Quantity One software (Bio-Rad).

Purification of HA-Flag-EYA1 and Myc-Cdh1 proteins. HA-Flag-EYA1 and Myc-Cdh1 were expressed in HEK293 cells by transient transfection, and the whole-cell lysates were immunoprecipitated using anti-FlagM2 beads or mouse anti-Myc antibody–protein A beads, respectively. After 5 washes in Tris-buffered saline (TBS) buffer, HA-Flag-tagged EYA1 protein was eluted with 3×Flag peptides, and the Myc-tagged Cdh1 protein was eluted with Myc peptide. The eluted proteins were frozen and stored at −80°C.

***Xenopus* egg extracts and destruction assay.** *Xenopus* cytostatic factor-arrested egg extracts (cerebrospinal fluid [CSF] extracts) were prepared as described previously (28, 29). Briefly, eggs from human chorionic gonadotropin (HCG)-injected frogs were collected and washed in 1× MMR (140 mM NaCl, 2.5 mM KCl, 1 mM $MgCl_2$, 1 mM $CaCl_2$, 10 mM HEPES [pH 7.4]). Eggs were dejellied with 2% cysteine and then washed into extraction buffer containing protease inhibitors. A 1-min packing spin at 1,000 rpm was performed, followed by a crushing spin at 10,000 rpm. The cytoplasmic layer was collected and subjected to a clarifying spin, also at 10,000 rpm. The clarified cytoplasmic layer was collected. After addition of an energy-regenerating system, protease inhibitors, cytochalasin B, and glycerol to 4%, extracts were frozen in liquid nitrogen and stored at −80°C. In these extracts, cyclin B destruction, inactivation of maturation promoting factor, and inactivation of CSF can be triggered for cell cycle progression to G_1 phase by the addition of 0.4 mM $CaCl_2$. As Cdh1 is absent from the eggs that were arrested at second metaphase of meiosis and does not appear during embryonic development until the midblastula transition (30), *Xenopus* egg extracts do not show degradation of known Cdh1 substrates. However, a cell-free FZR/Cdh1-APC/C-dependent destruction assay was reconstituted by adding purified Myc-Cdh1 to interphase egg extracts.

RESULTS

EYA1 abundance is cell cycle dependent. To investigate whether EYA1 activity is cell cycle regulated, we first performed immunostaining to characterize its abundance in C2C12 mouse myoblast cells. Immunofluorescence staining of a population of replicating C2C12 cells revealed that the cells endogenously express EYA1 protein during mitosis, with highest levels at metaphase to telophase/cytokinesis (Fig. 1a). A similar observation was obtained with wild-type MEFs (Fig. 1e). No signal was detected in *Eya1*$^{-/-}$ MEFs by either immunostaining (Fig. 1f) or Western blot analysis (Fig. 1g), demonstrating the specificity of the EYA1 antibody.

Since we have generated an HEK293 cell line that stably overexpresses 3× Flag-tagged *Eya1* (named the B22 cell line), we used this cell line to characterize the mechanism involved in the cell cycle regulation of EYA1 protein. Immunofluorescence staining of B22 cells with anti-Flag antibody revealed stronger signals for Flag-EYA1 in mitotic cells (Fig. 2a), similar to the endogenous EYA1 observed in C2C12 cells and MEFs (Fig. 1) or HeLa cells (Fig. 2b), further suggesting that the EYA1 protein is regulated in a cell cycle-dependent manner.

To validate the immunofluorescence staining data, we next set out to detect EYA1 in synchronized cultures. After synchronization of B22 cells at prometaphase with nocodazole followed by release into the cell cycle, cells were collected at each time point and analyzed by immunoblotting. EYA1 levels were higher during mitosis and decreased as the cells entered G_1/S phase (Fig. 2c and e), whereas β-actin levels did not change throughout the cell cycle (Fig. 2c). Similar result was obtained with HeLa cells (data not shown).

To test whether the abundance of EYA1 protein levels correlates with its mRNA expression levels, we isolated total RNAs from the cells that were synchronously progressing through the cell cycle by nocodazole treatment and performed semiquantitative RT-PCR for detecting *Eya1* transcripts. In contrast to the regulation of its protein levels, the levels of *Eya1* mRNA were comparable between the different treatments (Fig. 2d and e), similar to that of the 18S rRNA, which was used as an internal control (Fig. 2d and e).

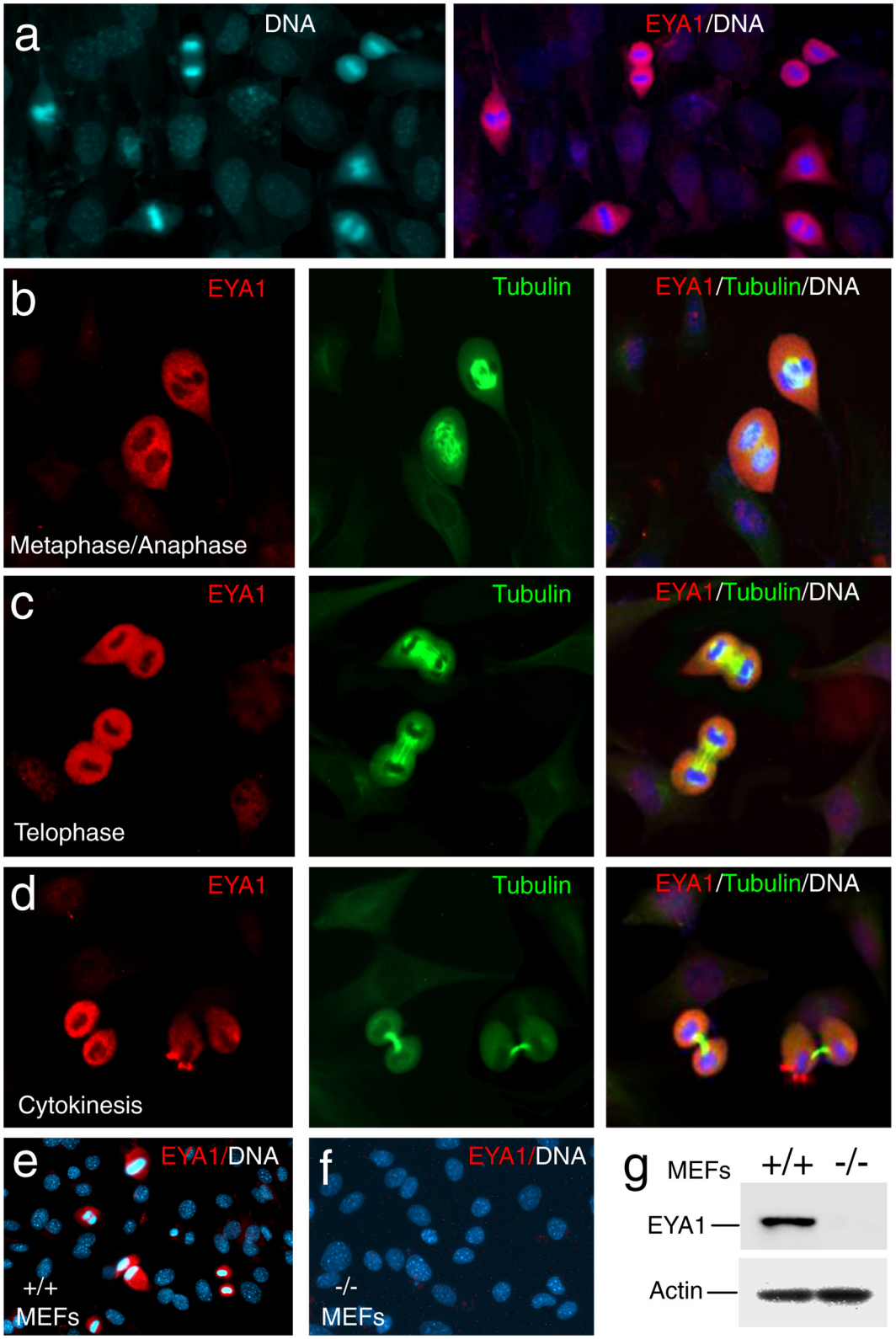

FIG 1 Levels of EYA1 protein are highest from metaphase to telophase. (a to d) C2C12 cells were coimmunostained with anti-EYA1 (red) and anti-α-tubulin (green) and counterstained with Hoechst (blue) to label the nucleus. High levels of EYA1 were detected in metaphase/anaphase (a and b), telophase (a and c), and cytokinesis (a and d). (e and f) Immunostaining showing EYA1 (red) in mitotic wild-type MEFs (e) and no expression in *Eya1*$^{-/-}$ MEFs (f). Hoechst (blue) was used to label the nucleus. (g) Western blot analysis of cell lysates prepared from wild-type and *Eya1*$^{-/-}$ MEFs. β-Actin was used as the loading control.

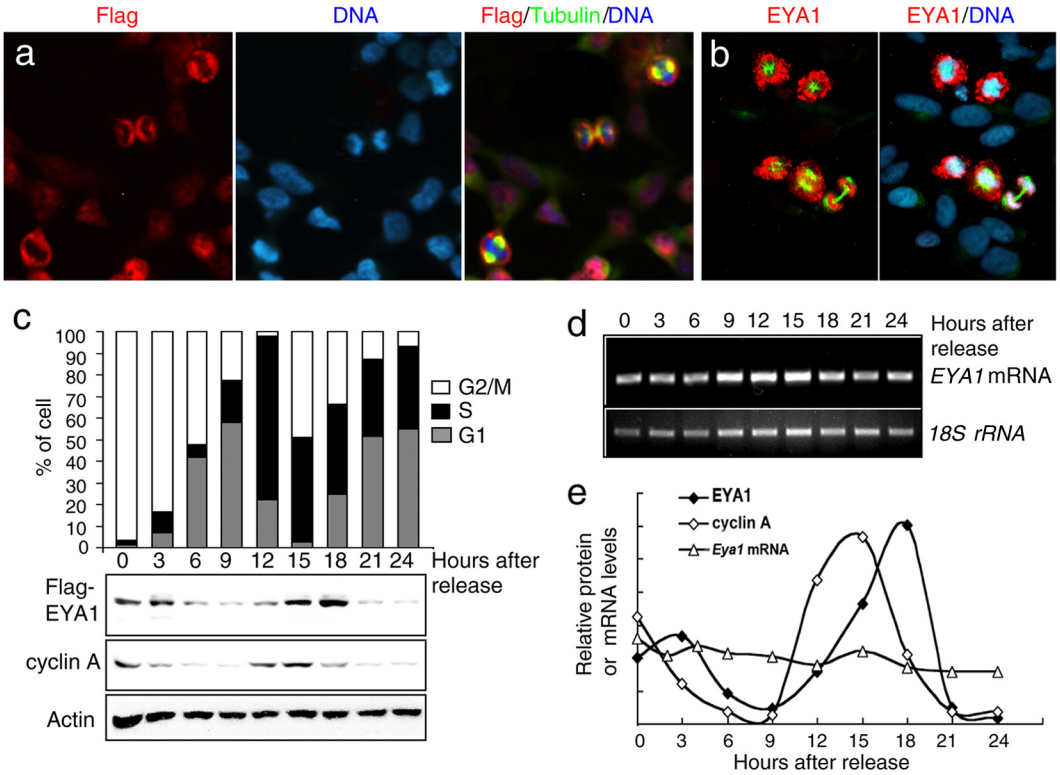

FIG 2 EYA1 abundance is cell cycle dependent. (a and b) Immunostaining of the B22 cells stably expressing *Flag-Eya1* with anti-Flag (a) or HeLa cells with anti-EYA1 (b) (red) and anti-α-tubulin (green) antibodies and counterstained with Hoechst (blue). (c) EYA1 protein levels decrease at M-to-G_1 transition. The B22 cells were arrested at the G_2/M phase by nocodazole treatment, released into fresh medium, and harvested at the indicated times. Cell lysates were subjected to Western blot assays with antibodies specific to Flag-tag and cyclin A. β-Actin was used as a loading control. Cell cycle status at various time points following release from nocodazole treatment was determined by flow cytometry. (d) *Eya1* mRNA levels at various time points following release from nocodazole treatment were analyzed using semiquantitative RT-PCR. 18S rRNA was used as an internal control. (e) Quantification of the levels of EYA1 protein, cyclin A protein, and *Eya1* mRNA.

Together, these data indicate that EYA1 is a cell cycle-regulated protein with highest levels during mitosis.

EYA1 can be ubiquitinated and degraded through the ubiquitin-proteasome pathway. To gain insight into the mechanisms regulating EYA1 protein stability, we investigated the involvement of ubiquitin ligases in EYA1 degradation. We first examined whether EYA1 is polyubiquitinated *in vivo*. HEK293 cells were cotransfected with *Flag-Eya1* and *HA-ubiquitin* expression plasmids. CoIP analysis of cell lysates prepared from the transfected cells with anti-Flag or anti-HA antibody revealed ubiquitinated forms of EYA1 (Fig. 3a). When *HA-ubiquitin* was transfected with an empty vector, no product was detected with either anti-HA or anti-Flag antibody (Fig. 3a).

To determine which region of the EYA1 protein mediates ubiquitination, we tested the deletion mutant construct containing either the N-terminal transactivation domain (*Flag-Eya1N*) or the C-terminal Eya domain (*Flag-Eya1D*). As shown in Fig. 3b, the ubiquitinated form of EYA1 was significantly reduced when the conserved Eya domain was deleted, whereas deletion of the N-terminal domain only slightly reduced the level of ubiquitinated EYA1 (Fig. 3b). Thus, the ubiquitination of EYA1 appears to be mediated by the conserved Eya domain.

We next investigated whether inhibition of the proteasome would increase the steady-state levels of EYA1 in mitotic cells. We first measured the EYA1 protein levels from HEK293 B22 cells that stably express *Flag-Eya1* in the absence or presence of the specific proteasome inhibitor MG132. We found that the levels of EYA1 protein were increased in the presence of MG132 (Fig. 3c). In contrast to HEK293 cells, EYA1 protein was almost undetectable 36 h after transfection into NIH 3T3 cells in the absence of MG132 (Fig. 3d). However, an accumulation of EYA1 protein was evident after treatment with MG132 (Fig. 3d). Although deletion of the Eya domain diminished the level of ubiquitination (Fig. 3b), we found that the stability of EYA1N or EYA1D was also increased in the presence of MG132 (Fig. 3d). This result indicates that similar to the full-length EYA1, the truncated EYA1N or EYA1D can also be degraded through the ubiquitin-proteasome pathway.

To determine the half-life of EYA1 protein, we treated the 3T3 cells transfected with *2×HA-3×Flag-Eya1* with cycloheximide (CHX). Since, in the absence of MG132, EYA1 was almost undetectable 24 to 36 h after transfection by Western analysis (Fig. 3d), we treated the *Eya1*-transfected cells with MG132 for 6 h and then washed out the drug and released the cells to normal medium in the presence of CHX. EYA1 degradation occurred after 90 min of CHX treatment (Fig. 3e), and its half-life was ~98 min (Fig. 3f).

To further confirm a role of Cdh1 in the proteolysis of EYA1, we performed *in vivo* ubiquitination assays. 3T3 cells were transfected with *HA-ubiquitin* and *Flag-Eya1* expression vectors along with empty vector or *Myc-Cdh1*. Twenty-four hours after transfection, cells were treated with MG132 for 6 h, and protein extracts

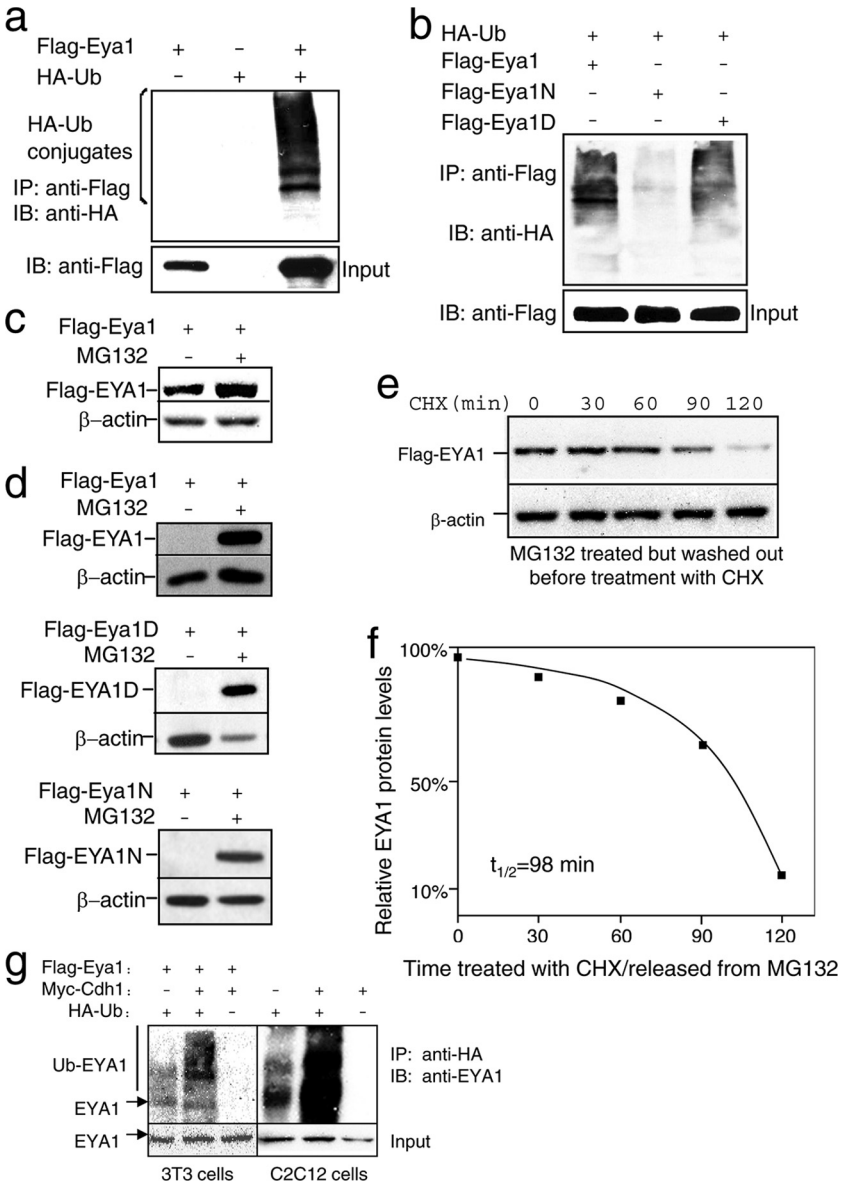

FIG 3 EYA1 is ubiquitinated and degraded through the ubiquitin-proteasome system. (a) CoIP and Western assays of lysates from HEK293 cells transiently cotransfected with *Flag-Eya1* and *HA-Ub* constructs using anti-Flag for immunoprecipitation (IP) and anti-HA for Western immunoblot detection (IB). Total input was detected by anti-Flag. (b) Ubiquitination of EYA1 is mediated by the conserved Eya domain. Cell lysates from HEK293 cells transiently transfected with *HA-Ub* and *Flag-Eya1*, *Flag-Eya1N*, or *Flag-Eya1D* were immunoprecipitated by anti-Flag and detected by anti-HA or -Flag by Western blot analysis. (c) EYA1 degradation in HEK293 cells can be protected in the presence of MG132. (d) EYA1 (full length), EYA1N, or EYA1D is also degraded in 3T3 cells, and their degradation can be protected in the presence of MG132. Lysates from 3T3 cells transiently transfected with *Flag-Eya1*, *Flag-Eya1N*, or *Flag-Eya1D* in the absence or presence of MG132 were analyzed by Western blot analysis with anti-Flag antibody. β-Actin was used as a loading control. (e) Western analysis of EYA1 levels using lysates from 3T3 cells transiently transfected with *Flag-Eya1*, treated with MG132 for 6 h, and then released to normal medium in the presence of CHX. (f) Quantification of data shown in panel e. The levels of EYA1 protein at each time point were quantified against β-actin levels using a densitometer, and the protein level at time zero was designated 100%. This experiment was repeated three times and the result was consistent. The half-life of EYA1 is ~98 min. (g) Cdh1-stimulated ubiquitination of the EYA1 protein *in vivo*. 3T3 cells were transfected with *Flag-Eya1* along with *HA-Ub* and/or *Myc-Cdh1* or empty vector, while C2C12 cells were transfected with *HA-Ub* or *Myc-Cdh1* alone or a combination of both. Cell lysates were bound to HA beads, and the bound fractions were analyzed for polyubiquitination of the EYA1 protein by Western blotting with anti-EYA1. Total input was detected by anti-EYA1.

were bound to HA beads to bind the ubiquitinated proteins. The levels of ubiquitinated EYA1 protein were analyzed by Western blot analysis using anti-EYA1 antibody. As shown in Fig. 3g, overexpression of Cdh1 caused a significant increase in the ubiquitination of EYA1. Similarly, overexpression of Cdh1 in C2C12 cells increased the ubiquitination levels of the endogenous EYA1 (Fig. 3g). Thus, overexpression of Cdh1 appears to promote ubiquitination of EYA1 *in vivo*.

Overexpression of Cdh1 reduces EYA1 levels. During the process of ubiquitination, ubiquitin is activated by E1 enzyme and transferred to ubiquitin-conjugating enzyme E2, which interacts with a specific E3 ligase and transfers the ubiquitin to the target

protein. The E3 ubiquitin ligase targets specific protein substrates for degradation by the proteasome. The APC/C ubiquitin ligase normally regulates exit from mitosis and events in G_1 (31) and is targeted to appropriate substrates by the evolutionarily conserved coactivators Cdc20/Fizzy in anaphase and Cdh1/FZR proteins from mitotic exit and in G_1, respectively (32). The downregulation of EYA1 after cytokinesis, when the APC/C-Cdh1 is most active, led us to test whether this ubiquitin ligase also regulates the G_1 levels of EYA1. We transfected and measured the levels of EYA1 by Western blotting. Interestingly, ectopically expressed EYA1 protein was decreased in the presence of Cdh1, whereas ectopically expressed Cdc20 had no or a very mild, if any, effect on coexpressed EYA1 levels (Fig. 4a). Overexpression of Cdh1 but not Cdc20 in C2C12 cells similarly reduced the levels of endogenous EYA1 (Fig. 4a). This result suggests that the APC/C-Cdh1 complex plays a role in ubiquitin-mediated turnover of EYA1. It should be noted that overexpression of Cdh1 but not Cdc20 impaired G_1-to-S transition (Fig. 4a). This result is consistent with previous observation that overexpression of Cdh1 causes a delay in S-phase onset and reduces the rate of DNA replication (33).

Cdh1 physically interacts with EYA1 and stimulates its degradation. We next determined whether EYA1 physically interacts with Cdh1. Cell lysates were prepared from HEK293 cells 24 h after transfection of *Flag-Eya1* together with *Myc-Cdc20* or *Myc-Cdh1* and were subjected to coIP analysis using either Flag or Myc epitope tag antibody. Flag-EYA1 and Myc-Cdh1 were coprecipitated by either anti-Myc or -Flag antibody, indicating a specific interaction between these two proteins (Fig. 4b). However, no interaction was found between EYA1 and Cdc20 (Fig. 4b). Deletion of the N-terminal or the C-terminal domain of EYA1 demonstrated that the EYA1-Cdh1 interaction was mediated by the conserved Eya domain (Fig. 4c).

CoIP analysis of cell lysates prepared from C2C12 cells using anti-EYA1 coprecipitated the endogenous FZR (Fig. 4d). Conversely, anti-FZR also coprecipitated the endogenous EYA1 (Fig. 4d). Consistent with the coIP analysis (Fig. 4c), *in vitro* glutathione *S*-transferase (GST) pulldown assay confirmed that purified GST-EYA1 (full length) or GST-EYA1D, but not GST-EYA1N, fusion protein directly interacted with the purified Myc-Cdh1 (Fig. 4e).

Cdh1 enhances the destruction of EYA1 *in vitro*. To test if EYA1 is an APC/C substrate, we purified 2×HA-3×Flag-EYA1 and Myc-Cdh1 proteins and set up an FZR/Cdh1-dependent destruction assay in *Xenopus* extracts as previously described (29) (Fig. 5a). Since the activity of Fizzy/Cdc20-APC/C was very low at 2 h after the addition of $CaCl_2$ to CSF extracts and endogenous FZR/Cdh1 was absent from *Xenopus* egg extracts (30), addition of recombinant Cdh1 to the interphase extracts results in activation of Cdh1-dependent APC/C. As shown in Fig. 5b, upon addition of Cdh1, EYA1, which was protected by MG132, was degraded after 30 min and almost completely destroyed after 2 h (data not shown). In the absence of Cdh1, EYA1 was relatively stable. This further indicates that EYA1 is a substrate for APC/C-Cdh1.

Silencing of Cdh1 stabilizes EYA1 *in vivo*. To confirm that the APC/C-Cdh1 complex is required for the destruction of EYA1 *in vivo*, we depleted the endogenous FZR/Cdh1 activity using *Fzr/Cdh1* shRNA. Cotransfection of *Fzr/Cdh1* shRNA but not control scramble shRNA together with *HA-Flag-Eya1* into 3T3 cells reduced the endogenous FZR/Cdh1 levels, which in turn not only led to an increase in the levels of EYA1 protein (Fig. 5c) but also stabilized the EYA1 protein (Fig. 5d). Similarly, knocking down FZR/Cdh1 activity in C2C12 cells resulted in a dramatic increase in the levels of EYA1 protein (Fig. 5e). Depletion of endogenous FZR/Cdh1 by shRNA transfection in either 3T3 or C2C12 cells also caused a severe inhibition of the ubiquitination of EYA1 (Fig. 5f). Immunostaining revealed a large increase in the number of $EYA1^+$ cells when FZR was depleted in C2C12 cells (Fig. 5g). Together, these data suggest that depletion of endogenous FZR/Cdh1 activity leads to stabilization of the EYA1 protein.

We next confirmed the role of Cdh1 in the early G_1 proteolysis of EYA1 following release from nocodazole arrest. C2C12 cells were transfected with control and *FZR/Cdh1* shRNA, respectively, and then arrested in G_2/M phase by treatments with nocodazole. At the indicated time points following release from nocodazole arrest, the cells were harvested and the extracts were assayed for EYA1 (Fig. 6). As expected, the cells expressing control shRNA exhibited a reduction in the levels of EYA1 in early G_1 phase, whereas the cells expressing *shFZR/Cdh1* did not show a reduction of EYA1 following release from the G_2/M-phase block (Fig. 6). Together, our data suggest a role of Cdh1 in the degradation of EYA1 in the late M and early G_1 phases of the cell cycle.

EYA1 degradation is independent of D-box and O-box motifs. Cdh1 recognizes specific motifs in the substrates: the destruction box (D-box; RXXL), O-box (LXXXN), or KEN box. The murine EYA1 contains one D-box within the Eya domain region at amino acids 322 to 325 (RVLL) and two O-boxes, one within the N-terminal region at amino acids 194 to 198 (LYSGN; O-box1) and the other within the Eya domain at amino acids 398 to 402 (LSTYN; O-box2) (Fig. 7a), but no KEN box. O-box2 is conserved among different species, whereas D-box or O-box1 is not. To determine whether the putative D-box and O-boxes of EYA1 are functional, we mutagenized those sites by changing the D-box RXXL to AXXA and O-box LXXXN to AXXXA (Fig. 7a). All three mutant forms were unstable when transfected into 3T3 cells, which can be protected by MG132 (Fig. 7b). In addition, combinations of all mutations at sites O-box1, D-box, and O-box2 did not stabilize EYA1 (Fig. 7b). This is consistent with the observation that deletion of the N or the C terminus of EYA1 did not stabilize the protein. Furthermore, addition of Cdh1 also appeared to enhance degradation of the mutant proteins (Fig. 7c). The half-life for all three mutants is similar to that of the wild-type EYA1 protein (Fig. 7d and e and data not shown), and depletion of endogenous FZR similarly stabilized the mutant proteins (data not shown). Thus, our results suggest that EYA1 contains novel degradation signals that are recognized by APC/C-Cdh1.

DISCUSSION

In this study, we aimed to investigate how EYA1 activity is regulated during an ongoing cell cycle. Our findings provide evidence that EYA1 is ubiquitinated and degraded during mitotic exit via the ubiquitin-proteasome pathway. This degradation requires the activity of APC/C-Cdh1 both *in vivo* and *in vitro* (Fig. 5b), thus identifying proteolysis as an important component of EYA1 protein regulation during an ongoing cell cycle.

EYA1 accumulates in the M phase, and its levels decrease as cells enter the G_1 phase. This profile of EYA1 is consistent with APC/C-Cdh1-mediated proteolysis. The APC/C-Cdh1 complex recognizes target proteins containing specific motifs, i.e., the D-box, KEN box, and O-box. Two of these motifs are found in the mouse EYA1. However, these known motifs are not critical for targeting by Cdh1, as mutating either motif had no effect on its

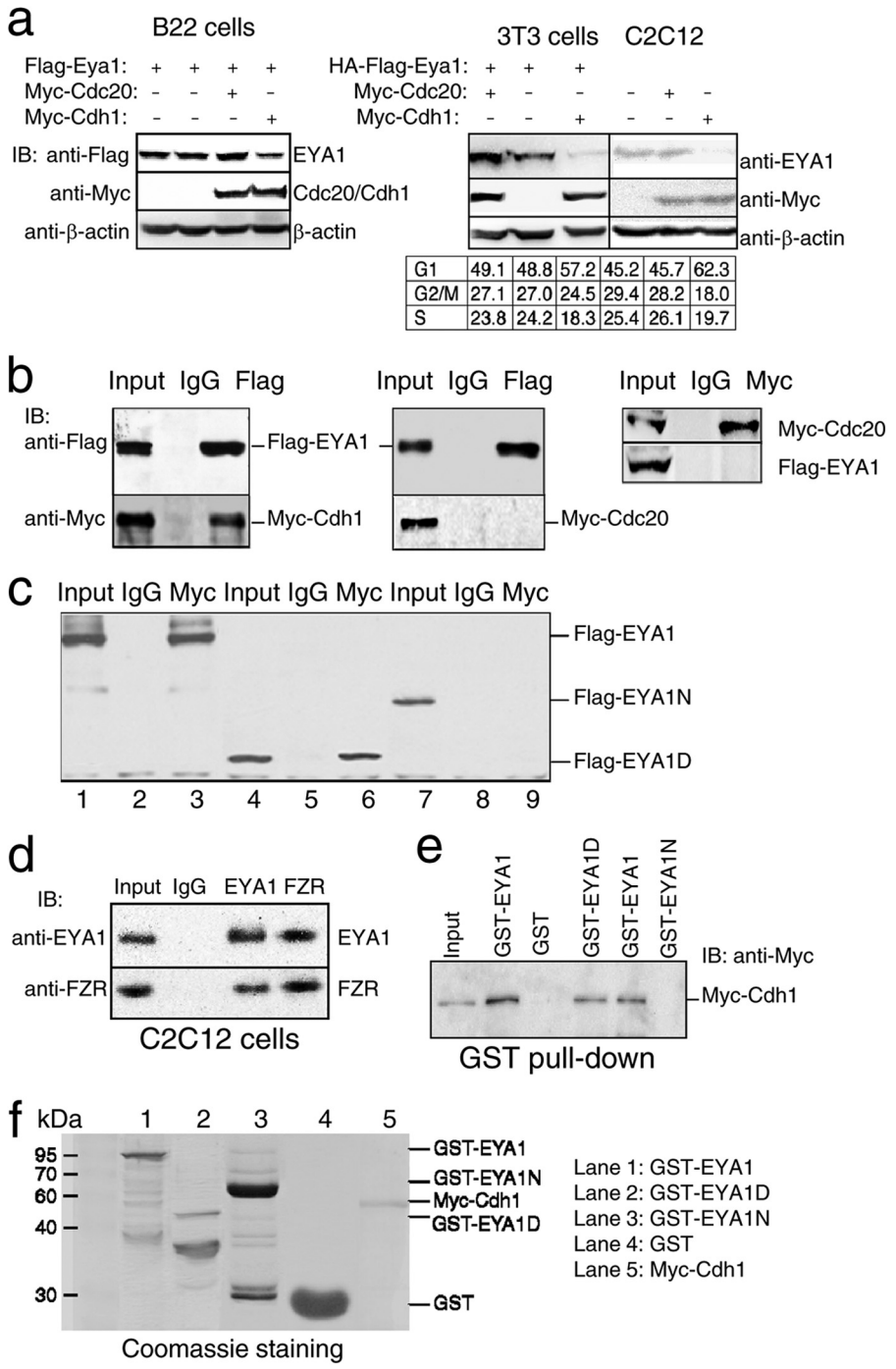

FIG 4 Cdh1 enhances EYA1 degradation and physically interacts with EYA1. (a) Western analysis of EYA1, Cdc20, or Cdh1 proteins in B22 cells stably expressing *Flag-Eya1*, 3T3 cells transfected with *HA-Flag-Eya1*, or C2C12 cells transfected with an empty vector, *Myc-Cdc20* or *Myc-Cdh1*. Data from a flow cytometry analysis of the transfected 3T3 or C2C12 cells are shown. (b) CoIP analysis of HEK293 cells transiently transfected with *Flag-Eya1* and *Myc-Cdc20* or *Myc-Cdh1* showing that EYA1 physically interacts with Cdh1 but not Cdc20. Anti-Flag or -Myc was used for IP or Western blotting. IgG was used as a negative control for this experiment. (c) Cdh1 specifically interacts with the conserved Eya domain. HEK293 cells were transiently cotransfected with *Myc-Cdh1* and *Flag-Eya1* (lane 1 to 3), *Flag-Eya1D* (lane 4 to 6), or *Flag-Eya1N* (lane 7 to 9). (d) CoIP analysis. Anti-EYA1 and -FZR were used for immunoprecipitation and Western blot analysis, respectively. IgG was used as a negative control. One-tenth of the amount used for coIP was loaded as the input. (e) GST pulldown assay. Purified Myc-Cdh1 and different GST proteins were incubated and then pulled down by GST beads and detected by anti-Myc antibody by Western blot analysis. (f) Coomassie staining showing different purified proteins.

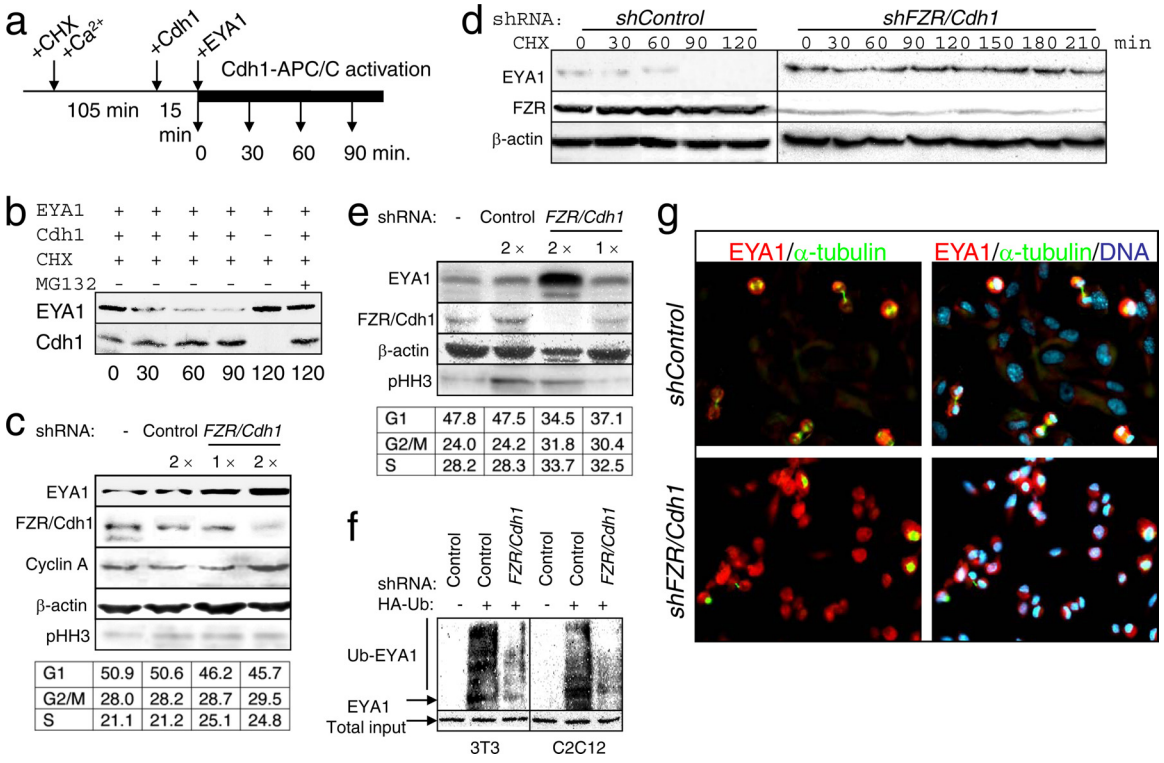

FIG 5 Cdh1 enhances destruction of EYA1 *in vitro*, and silencing of Cdh1 stabilizes EYA1 *in vivo*. (a) Schematic of a cell-free Cdh1-APC/C-dependent destruction assay constituted in *Xenopus* egg extracts. $CaCl_2$ and CHX were added into *Xenopus* extracts and incubated at 23°C for 105 min to release CSF arrest into interphase. Purified Myc-Cdh1 then was added to activate the interphase APC/C and after 15 min of incubation with Cdh1, substrate (HA-Flag-EYA1) was added at time zero, and samples were taken at the indicated time. CHX was added to prevent protein synthesis. (b) EYA1 is destroyed in a Cdh1-dependent destruction assay. The levels of HA-Flag-EYA1 were measured by Western blotting using anti-Flag in the presence or absence of Cdh1, CHX, or MG132. Myc-Cdh1 was detected by anti-Myc antibody. (c) Silencing FZR/Cdh1 increases the levels of EYA1 in 3T3 cells. The levels of EYA1 protein were measured in 3T3 cells transiently transfected with *HA-Flag-Eya1* alone or together with control shRNA (*shControl*) or *FZR/Cdh1* shRNA (*shFZR/Cdh1*) at two different concentrations. FZR/Cdh1 protein was detected using anti-FZR. Anti-cyclin A was used as a positive control, which is also a substrate of APC/Cdh1. Anti-pHH3 was used as a control for cells at prophase to metaphase. Data from a flow-cytometric analysis of the shRNA-transfected and untransfected cells are shown. (d) EYA1 is stable even after 3.5 h of treatment with CHX in 3T3 cells when FZR/Cdh1 activity was depleted by *FZR/Cdh1* shRNA but not control shRNA. The cells were cotransfected with *HA-Flag-Eya1* and control or *FZR/Cdh1* shRNA and treated with CHX. (e) Silencing FZR/Cdh1 in C2C12 cells also stabilizes EYA1 levels. EYA1 levels were measured using anti-EYA1 in untransfected cells or transiently transfected with control or *FZR/Cdh1* shRNA. Endogenous FZR protein was detected by anti-FZR. Anti-pHH3 was used as a control for cells at prophase to metaphase. β-Actin was used as a loading control. Data from a flow-cytometric analysis of the shRNA-transfected and untransfected cells are shown. (f) Silencing FZR/Cdh1 inhibits ubiquitination of exogenous and endogenous EYA1. 3T3 cells were cotransfected with *Flag-Eya1* and *HA-Ub* or an empty vector together with control or *FZR/Cdh1* shRNA. C2C12 cells were transfected with *HA-Ub* or an empty vector together with control or *FZR/Cdh1* shRNA. Cell lysates were bound to HA beads, and the bound fractions were analyzed with anti-EYA1 by Western blotting. Total input was detected by anti-EYA1. (h) Immunostaining showing high levels of EYA1 (red) in mitotic cells, labeled by α-tubulin (green) in C2C12 cells transfected with control shRNA, and increased levels of EYA1 in interphase cells transfected with *FZR/Cdh1* shRNA.

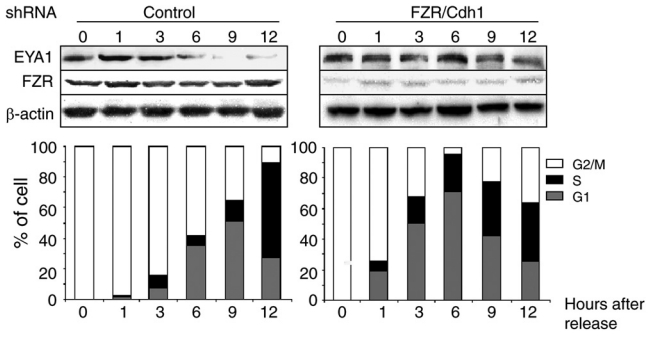

FIG 6 Depletion of Cdh1 in C2C12 cells by shRNA transfection inhibits reduction of EYA1 protein levels in late mitosis and G_1 phase of the cell cycle. C2C12 cells transfected with control or *FZR/Cdh1* shRNA were arrested in prometaphase by nocodazole, released, and then harvested at the indicated times following removal of nocodazole. Cell extracts were subjected to Western blot analysis with anti-EYA1 and -FZR. β-Actin was used as a loading control. Data from a flow-cytometric analysis of the shRNA-transfected and untransfected cells are shown.

interaction with Cdh1 and degradation by APC/C-Cdh1, suggesting that novel APC/C-Cdh1-targeting motifs exist. This is not unexpected, as a similar observation was previously described for several cell cycle regulators (34, 35). It is noteworthy that SIX1, the DNA-binding protein and cofactor of EYA1, is also degraded in a pathway involving APC/C-Cdh1 in a cell cycle-dependent manner, and its degradation is also independent of known APC degradation motifs (35). Previous studies have suggested that substrates lacking canonical D-boxes contain a three-dimensional interaction surface similar to a D-box but with a different primary amino acid sequence (36). Our results show that deletion of either the N or the C terminus does not stabilize EYA1 from degradation. Thus, an additional destruction sequence may be present in the N terminus. Since the N terminus does not appear to interact with Cdh1 and is only weakly ubiquitinated (Fig. 3b), it is possible that the proteolysis signal of EYA1 within the N terminus is not the same for APC/C-Cdh1. It should be noted that EYA1 is relatively

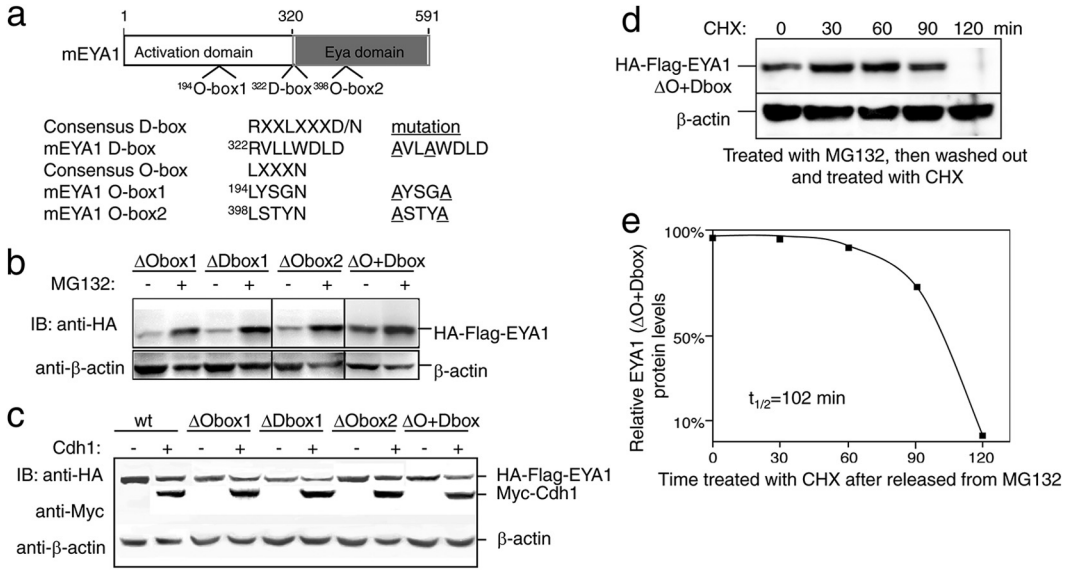

FIG 7 EYA1 degradation is independent of D-box and O-box motifs. (a) Schematic showing the putative D- and O-boxes in the mouse EYA1 and mutations introduced into D-box, O-box1, and O-box2. (b) Western blot of lysates from HEK293 cells transfected with the indicated constructs showing EYA1 levels in the absence or presence of MG132. β-Actin was used as a loading control. (c) Cdh1 enhances degradation of EYA1 wild-type or mutant proteins in HEK293 cells. Western blot analysis of lysates from cells transfected with the indicated *Eya1* wild-type or mutant constructs in the absence or presence of *Cdh1* construct. (d) Western analysis of the mutant EYA1 (containing all three mutations) levels using lysates from 3T3 cells transfected with *HA-Flag-Eya1ΔO+Dbox*. Twenty-four hours after transfection, the cells were treated with MG132 for 6 h, and then we washed out the drug and released the cells to normal medium in the presence of CHX. (e) Quantification of data shown in panel c. The levels of the protein at each time point were quantified against β-actin levels using a densitometer, and the protein level at time zero was designated 100%. The half-life of the mutant EYA1 is ~102 min.

stable in HEK293 cells compared to NIH 3T3 cells. Although the underlying mechanisms are unclear, a likely explanation is that EYA1 degradation involves some unknown factors which are differentially expressed in different cell lines. Furthermore, it is currently unclear whether EYA1 is targeted by a second E3 ligase at interphase, since APC/Cdh1 is active in G_1 but EYA1 levels are high only during M phase, or whether EYA1 is regulated at the translational level during M phase, since its mRNAs are expressed similarly throughout the cell cycle (Fig. 2d). Nonetheless, our observation that depleting Cdh1 stabilizes EYA1 protein throughout the cell cycle clearly indicates that APC/Cdh1 targets EYA1 for its degradation. A detailed study will be necessary to establish the degradation signal that targets the proteolysis of EYA1, to reveal the molecular details that mediate EYA1 degradation, and to determine whether EYA1 is targeted by a second E3 ligase or whether it is translationally regulated during M phase.

Eya1 is necessary for cell proliferation during mouse development, as loss of *Eya1* leads to reduced cell proliferation in several organ systems during mouse development (10, 12, 15, 37–39). Given that the levels of EYA1 are highest during mitosis, the loss of *Eya1* expression may lead to mitotic misregulation during the cell cycle, which in turn affects proliferation. Our data suggest that EYA1 acts through mitotic regulators, such as Cdc25B, to mediate mitotic progression, since we found that the expression of Cdc25B protein was largely diminished in $Eya1^{-/-}$ MEFs (data not shown).

EYA family proteins are found to be overexpressed in a subset of leukemia patients and in cancers of the lung, breast, prostate, cervix, and kidney (40, 41). EYA1 is capable of immortalizing hematopoietic progenitor cells *in vitro* and collaborates with its cofactor, SIX1, in hematopoietic transformation assays (41), while EYA2 and EYA1 are the key factors necessary for SIX1-mediated tumor progression in the breast (42). As SIX1 has been reported to be critical for G_2-M checkpoint control (43), it is possible that EYA activated in tumor cells contributes to the loss of cell cycle checkpoints and facilitates the rapid proliferation of these tumor cells. Loss of *Eya1* during development may cause cells to have a defective G_2-M checkpoint and to enter mitosis before repairing damaged DNA or increase cell susceptibility to DNA damaging, thus leading to death after cell division. Consistent with this view, abnormal cell death was observed in multiple organs in *Eya1*-deficient mice.

In conclusion, APC/Cdh1-mediated destruction of EYA1 provides a novel mechanism for controlling EYA1 levels in the cell cycle. Further genetic analysis is necessary to address its specific role under certain conditions, especially in some developmental stages and cell lineages. Identification of specific binding partners and targets of EYA1 during mitosis will be essential to understand its precise function during the cell cycle.

ACKNOWLEDGMENTS

We thank L. Zhu at Albert Einstein College of Medicine and P. Warburton and S. Sokol at Mount Sinai School of Medicine for helpful discussions and kindly sharing reagents, M. W. Kirschner at Harvard Medical School for kindly providing constructs, and C. Cheng and F. Wang for technical assistance.

This work was supported by NIH RO1 DK064640 and DC005824 (P.-X.X.), and K.I. was supported by NIH RO1 NS40972 (S.S.).

We declare no conflict of interest.

REFERENCES

1. **Li X, Oghi KA, Zhang J, Krones A, Bush KT, Glass CK, Nigam SK, Aggarwal AK, Maas R, Rose DW, Rosenfeld MG.** 2003. Eya protein

phosphatase activity regulates Six1-Dach-Eya transcriptional effects in mammalian organogenesis. Nature **426**:247–254.
2. **Rayapureddi JP, Kattamuri C, Steinmetz BD, Frankfort BJ, Ostrin EJ, Mardon G, Hegde RS.** 2003. Eyes absent represents a class of protein tyrosine phosphatases. Nature **426**:295–298.
3. **Tootle TL, Silver SJ, Davies EL, Newman V, Latek RR, Mills IA, Selengut JD, Parlikar BE, Rebay I.** 2003. The transcription factor Eyes absent is a protein tyrosine phosphatase. Nature **426**:299–302.
4. **Xu PX, Cheng J, Epstein JA, Maas RL.** 1997. Mouse Eya genes are expressed during limb tendon development and encode a transcriptional activation function. Proc. Natl. Acad. Sci. U. S. A. **94**:11974–11979.
5. **Chen R, Amoui M, Zhang Z, Mardon G.** 1997. Dachshund and eyes absent proteins form a complex and function synergistically to induce ectopic eye development in Drosophila. Cell **91**:893–903.
6. **Ohto H, Kamada S, Tago K, Tominaga SI, Ozaki H, Sato S, Kawakami K.** 1999. Cooperation of six and eya in activation of their target genes through nuclear translocation of Eya. Mol. Cell. Biol. **19**:6815–6824.
7. **Pignoni F, Hu B, Zavitz KH, Xiao J, Garrity PA, Zipursky SL.** 1997. The eye-specification proteins So and Eya form a complex and regulate multiple steps in Drosophila eye development. Cell **91**:881–891.
8. **Abdelhak S, Kalatzis V, Heilig R, Compain S, Samson D, Vincent C, Weil D, Cruaud C, Sahly I, Leibovici M, Bitner-Glindzicz M, Francis M, Lacombe D, Vigneron J, Charachon R, Boven K, Bedbeder P, Van Regemorter N, Weissenbach J, Petit C.** 1997. A human homologue of the Drosophila eyes absent gene underlies branchio-oto-renal (BOR) syndrome and identifies a novel gene family. Nat. Genet. **15**:157–164.
9. **Buller C, Xu X, Marquis V, Schwanke R, Xu PX.** 2001. Molecular effects of Eya1 domain mutations causing organ defects in BOR syndrome. Hum. Mol. Genet. **10**:2775–2781.
10. **Xu PX, Adams J, Peters H, Brown MC, Heaney S, Maas R.** 1999. Eya1-deficient mice lack ears and kidneys and show abnormal apoptosis of organ primordia. Nat. Genet. **23**:113–117.
11. **Xu PX, Woo I, Her H, Beier DR, Maas RL.** 1997. Mouse Eya homologues of the Drosophila eyes absent gene require Pax6 for expression in lens and nasal placode. Development **124**:219–231.
12. **Xu PX, Zheng W, Laclef C, Maire P, Maas RL, Peters H, Xu X.** 2002. Eya1 is required for the morphogenesis of mammalian thymus, parathyroid and thyroid. Development **129**:3033–3044.
13. **Zou D, Silvius D, Fritzsch B, Xu PX.** 2004. Eya1 and Six1 are essential for early steps of sensory neurogenesis in mammalian cranial placodes. Development **131**:5561–5572.
14. **Sajithlal G, Zou D, Silvius D, Xu PX.** 2005. Eya 1 acts as a critical regulator for specifying the metanephric mesenchyme. Dev. Biol. **284**:323–336.
15. **Zou D, Silvius D, Rodrigo-Blomqvist S, Enerback S, Xu PX.** 2006. Eya1 regulates the growth of otic epithelium and interacts with Pax2 during the development of all sensory areas in the inner ear. Dev. Biol. **298**:430–441.
16. **Bonini NM, Leiserson WM, Benzer S.** 1993. The eyes absent gene: genetic control of cell survival and differentiation in the developing Drosophila eye. Cell **72**:379–395.
17. **Behbakht K, Qamar L, Aldridge CS, Coletta RD, Davidson SA, Thorburn A, Ford HL.** 2007. Six1 overexpression in ovarian carcinoma causes resistance to TRAIL-mediated apoptosis and is associated with poor survival. Cancer Res. **67**:3036–3042.
18. **Miller SJ, Lan ZD, Hardiman A, Wu J, Kordich JJ, Patmore DM, Hegde RS, Cripe TP, Cancelas JA, Collins MH, Ratner N.** 2010. Inhibition of eyes absent homolog 4 expression induces malignant peripheral nerve sheath tumor necrosis. Oncogene **29**:368–379.
19. **Pandey RN, Rani R, Yeo EJ, Spencer M, Hu S, Lang RA, Hegde RS.** 2010. The Eyes Absent phosphatase-transactivator proteins promote proliferation, transformation, migration, and invasion of tumor cells. Oncogene **29**:3715–3722.
20. **Zhang L, Yang N, Huang J, Buckanovich RJ, Liang S, Barchetti A, Vezzani C, O'Brien-Jenkins A, Wang J, Ward MR, Courreges MC, Fracchioli S, Medina A, Katsaros D, Weber BL, Coukos G.** 2005. Transcriptional coactivator Drosophila eyes absent homologue 2 is up-regulated in epithelial ovarian cancer and promotes tumor growth. Cancer Res. **65**:925–932.
21. **Cook PJ, Ju BG, Telese F, Wang X, Glass CK, Rosenfeld MG.** 2009. Tyrosine dephosphorylation of H2AX modulates apoptosis and survival decisions. Nature **458**:591–596.
22. **Deshaies RJ, Joazeiro CA.** 2009. RING domain E3 ubiquitin ligases. Annu. Rev. Biochem. **78**:399–434.
23. **Wickliffe K, Williamson A, Jin L, Rape M.** 2009. The multiple layers of ubiquitin-dependent cell cycle control. Chem. Rev. **109**:1537–1548.
24. **Visintin R, Prinz S, Amon A.** 1997. CDC20 and CDH1: a family of substrate-specific activators of APC-dependent proteolysis. Science **278**:460–463.
25. **Kramer ER, Scheuringer N, Podtelejnikov AV, Mann M, Peters JM.** 2000. Mitotic regulation of the APC activator proteins CDC20 and CDH1. Mol. Biol. Cell **11**:1555–1569.
26. **Zachariae W, Schwab M, Nasmyth K, Seufert W.** 1998. Control of cyclin ubiquitination by CDK-regulated binding of Hct1 to the anaphase promoting complex. Science **282**:1721–1724.
27. **Alkuraya FS, Saadi I, Lund JJ, Turbe-Doan A, Morton CC, Maas RL.** 2006. SUMO1 haploinsufficiency leads to cleft lip and palate. Science **313**:1751.
28. **Murray AW.** 1991. Cell cycle extracts. Methods Cell Biol. **36**:581–605.
29. **Pfleger CM, Kirschner MW.** 2000. The KEN box: an APC recognition signal distinct from the D box targeted by Cdh1. Genes Dev. **14**:655–665.
30. **Lorca T, Castro A, Martinez AM, Vigneron S, Morin N, Sigrist S, Lehner C, Doree M, Labbe JC.** 1998. Fizzy is required for activation of the APC/cyclosome in Xenopus egg extracts. EMBO J. **17**:3565–3575.
31. **Izawa, D, Pines J.** 2011. How APC/C-Cdc20 changes its substrate specificity in mitosis. Nat. Cell Biol. **13**:223–233.
32. **Peters JM.** 2002. The anaphase-promoting complex: proteolysis in mitosis and beyond. Mol. Cell **9**:931–943.
33. **Sorensen CS, Lukas C, Kramer ER, Peters JM, Bartek J, Lukas J.** 2000. Nonperiodic activity of the human anaphase-promoting complex-Cdh1 ubiquitin ligase results in continuous DNA synthesis uncoupled from mitosis. Mol. Cell. Biol. **20**:7613–7623.
34. **Castro A, Vigneron S, Bernis C, Labbe JC, Lorca T.** 2003. Xkid is degraded in a D-box, KEN-box, and A-box-independent pathway. Mol. Cell. Biol. **23**:4126–4138.
35. **Christensen KL, Brennan JD, Aldridge CS, Ford HL.** 2007. Cell cycle regulation of the human Six1 homeoprotein is mediated by APC(Cdh1). Oncogene **26**:3406–3414.
36. **Eytan E, Moshe Y, Braunstein I, Hershko A.** 2006. Roles of the anaphase-promoting complex/cyclosome and of its activator Cdc20 in functional substrate binding. Proc. Natl. Acad. Sci. U. S. A. **103**:2081–2086.
37. **Xu PX, Zheng W, Huang L, Maire P, Laclef C, Silvius D.** 2003. Six1 is required for the early organogenesis of mammalian kidney. Development **130**:3085–3094.
38. **Zheng W, Huang L, Wei ZB, Silvius D, Tang B, Xu PX.** 2003. The role of Six1 in mammalian auditory system development. Development **130**:3989–4000.
39. **Zou D, Erickson C, Kim EH, Jin D, Fritzsch B, Xu PX.** 2008. Eya1 gene dosage critically affects the development of sensory epithelia in the mammalian inner ear. Hum. Mol. Genet. **17**:3340–3356.
40. **Rhodes DR, Kalyana-Sundaram S, Mahavisno V, Varambally R, Yu J, Briggs BB, Barrette TR, Anstet MJ, Kincead-Beal C, Kulkarni P, Varambally S, Ghosh D, Chinnaiyan AM.** 2007. Oncomine 3.0: genes, pathways, and networks in a collection of 18,000 cancer gene expression profiles. Neoplasia **9**:166–180.
41. **Wang QF, Wu G, Mi S, He F, Wu J, Dong J, Luo RT, Mattison R, Kaberlein JJ, Prabhakar S, Ji H, Thirman MJ.** 2011. MLL fusion proteins preferentially regulate a subset of wild-type MLL target genes in the leukemic genome. Blood **117**:6895–6905.
42. **Farabaugh SM, Micalizzi DS, Jedlicka P, Zhao R, Ford HL.** 2012. Eya2 is required to mediate the pro-metastatic functions of Six1 via the induction of TGF-beta signaling, epithelial-mesenchymal transition, and cancer stem cell properties. Oncogene **31**:552–562.
43. **Ford HL, Landesman-Bollag E, Dacwag CS, Stukenberg PT, Pardee AB, Seldin DC.** 2000. Cell cycle-regulated phosphorylation of the human SIX1 homeodomain protein. J. Biol. Chem. **275**:22245–22254.